CHEMISTRY
A EUROPEAN JOURNAL

DOI: 10.1002/chem.200600352

Ca^{2+}– and Ba^{2+}–Ligand Coordinated Unilamellar, Multilamellar, and Oligovesicular Vesicles

Aixin Song,[a, b] Xiangfeng Jia,[a] Minmin Teng,[a] and Jingcheng Hao*[a, b]

Abstract: Ca^{2+}- and Ba^{2+}-coordinated vesicle phases were prepared in mixed aqueous solutions of tetradecyldimethylamine oxide (C_{14}DMAO) and calcium oleate ($Ca(OA)_2$) or barium oleate ($Ba(OA)_2$). At the right mixing ratios, metal–ligand coordination between $Ca(OA)_2$ or $Ba(OA)_2$ and C_{14}DMAO results in the formation of molecular bilayers due to the reduction in area per head group. Ca^{2+} and Ba^{2+} tightly associate to the head groups of surfactants and in this system the bilayer membranes are not shielded by excess salts. The structures of the birefringent samples of the $Ca(OA)_2/C_{14}$DMAO/H_2O and $Ba(OA)_2/C_{14}$DMAO/H_2O systems were determined by freeze-fracture transmission electron microscopy (FF-TEM), small-angle X-ray scattering (SAXS), and rheological measurements to consist of unilamellar, multilamellar, and oligovesicular vesicles. The coordination between C_{14}DMAO and $Ba(OA)_2$ or $Ca(OA)_2$ plays an important role in the formation of the vesicles, which was easily confirmed by studying the phase behavior of the KOA/C_{14}DMAO/H_2O system in which only the L_1 phase forms, due to the absence of coordination between KOA and C_{14}DMAO. A mechanism is proposed that accounts for the formation of these new metal–ligand coordinated vesicles.

Keywords: coordination modes · ligands · self-assembly · surfactants · vesicles

Introduction

Self-assembled structures of surfactants in solution have attracted much interest due to their potential applications in the fields of bionics, medicine, and materials science. Vesicles formed from amphiphilic molecules in aqueous solutions are fascinating self-assembled structures because they can be simple model systems for biological membranes[1] and templates for synthesizing novel materials.[2] Because vesicles made of phospholipids, such as lecithin, were first observed in biological systems, many routes to construct vesicle phases by using surfactants in aqueous solutions have been explored.[3] Based on general geometrical considerations of packing molecules into distinct aggregate shapes, surfactants can form bilayer membranes if the packing parameter P is in the range $\frac{1}{2} \leq P \leq 1$ ($P = \frac{al}{v}$, in which a is the interfacial area occupied by a surfactant headgroup and l and v are the length and volume of the hydrophobic group, respectively).[4] The driving forces for forming self-assemblies of surfactants include van der Waals forces, hydrophobic forces, hydrogen bonding, and screened electrostatic interactions.[5] In recent years, hydrogen bonding[6] and metal–ligand complexation[7] have been used as new noncovalent interactions in the engineering of supramolecular assemblies.

Cationic/anionic (catanionic) surfactant mixed systems are a most interesting and popular subject of investigation.[8–11] In catanionic aqueous solutions, the electrostatic interaction of the oppositely charged surfactants significantly reduces the headgroup areas, producing novel solution and interfacial properties, that is, aggregates can form at considerably lower concentrations than the critical micellar concentration (cmc) values of each individual surfactant. The properties and structures of bilayer membranes formed by catanionic surfactants in aqueous solutions have been widely studied[12] and, recently, particular self-assemblies, such as disklike micelles and regular hollow icosahedral aggregates, in "true" salt-free catanionic surfactant aqueous solutions have been observed by freeze-fracture transmission electron microscopy (FF-TEM), small-angle X-ray scattering (SAXS), and small-angle neutron scattering (SANS).[13–15] In the catanion-

[a] Dr. A. Song, X. Jia, M. Teng, Prof. Dr. J. Hao
Key Laboratory of Colloid and Interface Chemistry
Shandong University, Ministry of Education, Jinan 250100 (China)
Fax: (+86) 531-8856-4464
E-mail: jhao@sdu.edu.cn

[b] Dr. A. Song, Prof. Dr. J. Hao
State Key Laboratory of Solid Lubrication
Lanzhou Institute of Chemical Physics
Chinese Academy of Sciences, Lanzhou 730000 (China)

ic surfactant mixtures, many investigations have focused on mixtures of a cationic surfactant with a negatively charged ion, such as Br^- or Cl^-, as the counterion and an anionic surfactant with a positively charged ion, such as Na^+, K^+, or NH_4^+, as counterion. After mixing the cationic and anionic surfactants, the counterions remain in solution, inducing high conductivity. The excess salt screens the electrostatic interactions between the cationic and anionic surfactants. To prepare salt-free catanionic systems, we previously prepared "true", salt-free catanionic surfactant mixtures by using H^+ and OH^- as the counterions for the cationic and anionic surfactants, respectively, thereby forming water by the combination of the counterions. An onion phase was obtained in salt-free zero-charged catanionic surfactant solutions of tetradecyltrimethylammonium hydroxide (TTAOH) and oleic acid (OA).[16]

Metal–ligand interaction used in the formation of supramolecular links in traditional surfactant systems were investigated recently by us and Hoffmann.[17,18] In our work, the results concerning the Zn^{2+}–ligand complexes from the mixtures of zinc 2,2-dihydroperfluorooctanoate [$Zn(OOCCH_2C_6F_{13})_2$] and C_{14}DMAO (tetradecyldimethylamine oxide) in aqueous solution were presented. A charged surfactant–vesicle phase was prepared without any cosurfactant and the charges were not shielded because the solutions were salt-free. The vesicle phase was induced by Zn^{2+}–ligand coordination for which Zn^{2+} is the central ion and forms charged bilayers without counterions in the mixtures.

Herein we report the construction of a morphologically diverse vesicle phase in aqueous solution from a carboxylate surfactant with alkaline-earth counterions coordinated to a zwitterionic surfactant. By using the M^{2+}–ligand interaction, unilamellar, multilamellar, and oligovesicular vesicles were prepared with either calcium or barium oleate ($Ca(OA)_2$ or $Ba(OA)_2$) and C_{14}DMAO. The structure and properties were determined by FF-TEM, SAXS, and rheological measurements. The vesicle-formation mechanism, including models of unilamellar, multilamellar, and oligovesicular vesicles, is presented. To demonstrate the coordination of Ca^{2+} and Ba^{2+}, the phase behavior of potassium oleate (KOA) and C_{14}DMAO were investigated. The purpose of the present study is to prepare "true" salt-free surfactant mixtures with an ionically charged vesicle phase that is not shielded by excess salt in aqueous solutions,[9–12] thus, providing a new self-assembled template to prepare inorganic materials.

Results and Discussion

Phase behaviors of $Ca(OA)_2/C_{14}DMAO/H_2O$ and $Ba(OA)_2/C_{14}DMAO/H_2O$ systems: The phase behavior of 100 mmol L^{-1} C_{14}DMAO aqueous solutions with increasing concentrations of $Ca(OA)_2$ or $Ba(OA)_2$ up to ~40 mmol L^{-1} at 25.0 ± 0.1 °C is shown in Figure 1. The 100 mmol L^{-1} C_{14}DMAO aqueous solution is a low-viscosity L_1 phase (micellar solution, zero-shear viscosity, $|\eta^0|=1.98\times10^{-3}$ Pas) with very low conductivity ($\kappa=\sim100$ μS cm^{-1}). The solubility of $Ca(OA)_2$ or $Ba(OA)_2$ in water at room temperature is very low. Upon mixing with C_{14}DMAO solution, the Krafft point (higher than 80 °C) of $Ca(OA)_2$ or $Ba(OA)_2$ is clearly reduced. The two mixed systems have almost the same phase behaviors. As the amount of $Ca(OA)_2$ or $Ba(OA)_2$ increases, we observe single, clear L_1-phase solutions. The solutions have low viscosity and are composed of spherical micelles. Two-phase solutions, consisting of a slightly turbid viscous Lα phase at the bottom and a clear L_1 phase on top of the Lα phase, appear in the $Ca(OA)_2/C_{14}DMAO/H_2O$ system as the $Ca(OA)_2$ concentration increases from ~10 to ~16 mmol L^{-1}. In the $Ba(OA)_2/C_{14}DMAO/H_2O$ system, the phase separation was observed within a limited concentration range of ~7 to 9 mmol L^{-1}. By increasing the amount of $Ca(OA)_2$ or $Ba(OA)_2$, we obtained the slightly turbid viscous Lα phase for $Ca(OA)_2$ concentrations between ~16 and ~24 mmol L^{-1} or $Ba(OA)_2$ concentrations between ~9 and 17 mmol L^{-1}. The samples separate into L_1/precipitate phases as additional $Ca(OA)_2$ or $Ba(OA)_2$ is added. The upper phase is an isotropic L_1 phase and there are $Ca(OA)_2$ or $Ba(OA)_2$ precipitates in the bottom phase.

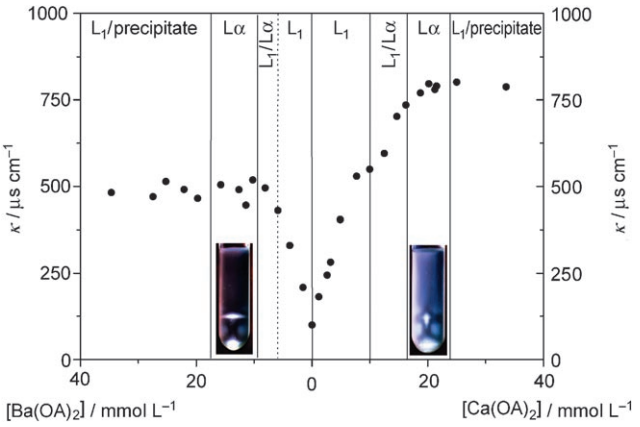

Figure 1. Phase diagram of 100 mmol L^{-1} C_{14}DMAO with different concentrations of $Ca(OA)_2$ and $Ba(OA)_2$ in aqueous solutions at $T=25.0\pm0.1$ °C. Conductivity data (●) are also shown. Inserts: photographs of Lα-phase samples for the two systems, taken with a polarizing filter.

The phase boundaries can also be determined by conductivity data (Figure 1). The 100 mmol L^{-1} C_{14}DMAO solution hardly ionizes and has very low conductivity values. As $Ca(OA)_2$ or $Ba(OA)_2$ are added, they undergo partial ionization and the conductivities increase more or less linearly as the amounts of $Ca(OA)_2$ or $Ba(OA)_2$ in the L_1 phase increase, up to the phase boundary at which the two-phase region begins. Upon reaching the Lα phase, the conductivities remain almost constant despite the addition of $Ca(OA)_2$ or $Ba(OA)_2$. This suggests that Ca^{2+} and Ba^{2+} tightly associate to the head groups of the bilayer membranes. The phase behavior and the conductivity change in the $Ca(OA)_2/C_{14}DMAO/H_2O$ and $Ba(OA)_2/C_{14}DMAO/H_2O$ systems are similar to those of other catanionic surfactant mixtures in aqueous solutions.[19]

FF-TEM micrographs of Ca^{2+}– and Ba^{2+}–ligand coordinated vesicles: Ca^{2+}– and Ba^{2+}–ligand coordinated vesicles produced in the $Ca(OA)_2/C_{14}DMAO/H_2O$ and $Ba(OA)_2/C_{14}DMAO/H_2O$ systems were observed by FF-TEM microscopy (Figure 2). In both birefringent Lα-phase solutions, unilamellar, multilamellar, and oligovesicular vesicles are

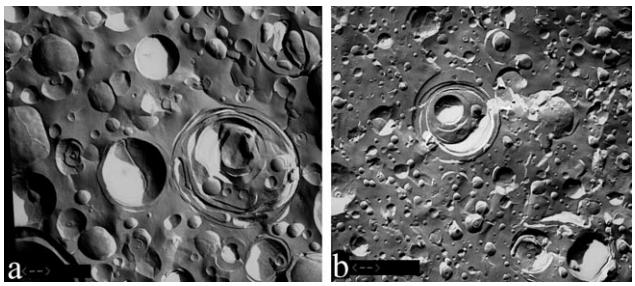

Figure 2. FF-TEM images of Lα-phase solutions for 100 mmol L^{-1} $C_{14}DMAO$ mixed with a) 20 mmol L^{-1} $Ca(OA)_2$ and b) 12 mmol L^{-1} $Ba(OA)_2$. Scale bars correspond to 0.350 μm.

observed, although oligovesicular vesicles with small uni- and multilamellar vesicles trapped inside are rare. The vesicles have rather polydisperse size distributions. In the $Ca(OA)_2/C_{14}DMAO/H_2O$ system (Figure 2a), the diameters of the unilamellar vesicles range greatly from around 50 to 500 nm, the multilamellar vesicle have diameters of more than 800 nm, and oligovesicular vesicles are much larger, at around 1.4 μm in diameter. For the $Ba(OA)_2/C_{14}DMAO/H_2O$ system (Figure 2b), the diameters of the unilamellar vesicles are similar to those in the Ca^{2+} system (around 50 to 600 nm), the multilamellar vesicles are around 500 nm in diameter, and the sizes of oligovesicular vesicles are similar to those in the Ca^{2+} system, with much larger diameters of more than 1 μm.

Small angle X-ray scattering (SAXS) measurements of Ca^{2+}– and Ba^{2+}–ligand coordinated vesicles: Scattering methods, such as X-ray, light, and neutron sources (in historical order) are the key techniques used to characterize the various morphologies and structures in systems containing colloids, polymers, surfactants, and biological macromolecules ("soft condensed matter"). The various morphologies and mesostructures obtained in aqueous surfactant solutions, including globules, such as globular micelles (L_1 phase); cylinders, such as hexagonal structures with cylindrical assemblies (crystallized in a hexagonal lattice); bilayers with various topologies on large scales, such as infinite flat bilayers (Lαh); vesicles (Lαv or L_4 phase); and multiconnected bilayers (L_3 phase) have been characterized by using scattering techniques.[20,21] By neglecting the interactions involved, we can suppose that vesicles have unilamellar spherical shells with internal and external radii R_i and R_o (shell thickness $\delta = R_o - R_i$). Normally, the high q region should be indicative of the structures of local aggregates present. This part of the scattering curve can be fitted well with the simple model of a lamellar structure and should also be valid for vesicle phases if they are treated as flat objects. The scattering intensity of lamellar structures can be represented by Equation (1):[20]

$$I(q) = \frac{2\pi}{q^2}\phi\delta(\Delta\rho)^2\left(\frac{\sin q\delta/2}{q\delta/2}\right)^2 \quad (1)$$

in which q is the scattering vector ($q = (4\pi/\lambda)\sin\theta/2$), ϕ is the volume fraction, $\Delta\rho$ is the difference in scattering-length density between the amphiphilic aggregates and the solvent, and δ is the shell thickness of bilayers.

SAXS scattering patterns (note that Figure 3 is on a logarithmic plot) for two birefringent Lα-phase sample solutions in Ca^{2+} and Ba^{2+} systems are shown in Figure 3. Two characteristics of the two SAXS curves are apparent: 1) the essentially identical scattering patterns suggest that the self-assembled structures formed in the two sample solutions are the same, 2) nonspecific scattering patterns were achieved and provide no direct evidence for the unilamellar, multilamellar, and oligovesicular vesicles demonstrated by FF-TEM images. However, in the high q-value region the curves display a q^{-2} dependence, demonstrating that a locally bilayered morphology must be present.[16] At lower q values, there is a progressive crossover towards a weaker dependence that is determined in a nonstraightforward manner by the system and the concentration of the sample.

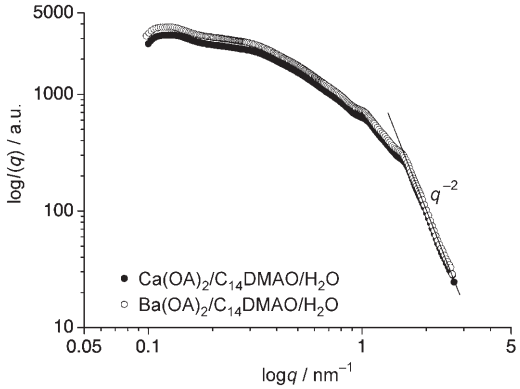

Figure 3. SAXS curves of Ca^{2+}– and Ba^{2+}–ligand coordinated vesicles for 100 mmol L^{-1} $C_{14}DMAO$ mixed with 20 mmol L^{-1} $Ca(OA)_2$ (●) and 12 mmol L^{-1} $Ba(OA)_2$ (○). $T = 25.0 \pm 0.1$ °C. The first position peak is expected to be at $q_{max} = 0.55$ nm^{-1}.

The main reasons for the nonspecific character of the static scattering are the polydispersity in vesicle size, a variety of ordered structures (i.e., unilamellar, multilamellar, and oligovesicular vesicles), the bilayer multiplicity of vesicles, and interbilayer distance. The static scattering alone cannot characterize unambiguously phases of polydisperse and morphologically diverse vesicles (i.e., unilamellar, multilamellar, and oligovesicular vesicles).[21] The two scattering curves show nonspecific scattering patterns because of the very disperse situation typical for the morphologically diverse vesi-

cles. This causes the maxima and minima peaks to be blurred and nothing specific can be exploited from the scattering. The bilayer thickness of unilamellar, multilamellar, and oligovesicular vesicles was determined to be around 25 A, according to the theoretical calculation for the lamellar-layer model [Eq. 1] from the high q-value region of the scattering spectra.[20] The value of 25 A for the bilayer thickness is much lower than one might expect for a bilayer of C_{18} and C_{14} surfactant, but one should keep in mind the possibility of tilt, random orientation, comb-shaped and enlaced arrangements of alkyl chains in membrane bilayers. These arrangements of alkyl chains, especially the comb-shaped and enlaced arrangements of alkyl chains in membrane bilayers, could explain the relative thinness of the vesicle shell and may also account for the possible vesicle formation of the proposed tetrachain, metal-coordinated complex (with such a geometry, how could the complex assemble into bilayers?). There was a weak scattering peak at around $q = 0.125\,nm^{-1}$, and an average interlamellar distance, that is, the lamellar thickness plus the interlamellar distance itself, of around 50 nm could be determined, which is consistent with the value reported for other systems that have a surfactant concentration of around $100\,mmol\,L^{-1}$.[17,18] Such a bilayer structure has been commonly observed in mixtures of amphiphilic block copolymer/water (or oil)[22] and cationic/anionic surfactant systems,[21,6b] however, no observations have been reported of such a bilayer structure for Ca^{2+}– or Ba^{2+}–ligand coordinated vesicles.

Rheological properties of Ca^{2+}– and Ba^{2+}–ligand coordinated vesicles: Comparative rheograms of the two birefringent Lα-phase sample solutions were quantitatively characterized and are shown in Figure 4. The sample solutions of birefringent Lα phase in Ca^{2+} and Ba^{2+} systems exhibit a yield stress that is demonstrated by air bubbles trapped in such samples. Two conclusions can be drawn from Figure 4: 1) The rheological parameters of the two samples are almost the same, consistent with the formation of similar structures, as demonstrated by the FF-TEM images and SAXS measurements. 2) The complex fluid behaves like a Bingham fluid with yield stress values. This is indicated by the fact that the storage modulus describing the elastic properties of the system and the loss modulus remain more or less constant at about 50 Pa and 5–6 Pa, respectively, over the whole frequency range investigated. The storage modulus is about one order of magnitude higher than the loss modulus, and the complex viscosities decrease over the whole frequency range from 0.01 to 10 Hz with a slope of −1, suggesting the presence of uni- and multilamellar vesicles.

Evidence of Ca^{2+}– and Ba^{2+}–ligand coordinated vesicles: Metal–ligand coordination between Ca^{2+} or Ba^{2+} and C_{14}DMAO would result in the reduction in area per head group, which, at the right mixing ratios, induces the formation of molecular bilayers. Evidence for the formation of Ca^{2+}– and Ba^{2+}–ligand coordinated unilamellar, multilamellar, and oligovesicular vesicles was obtained by studying the

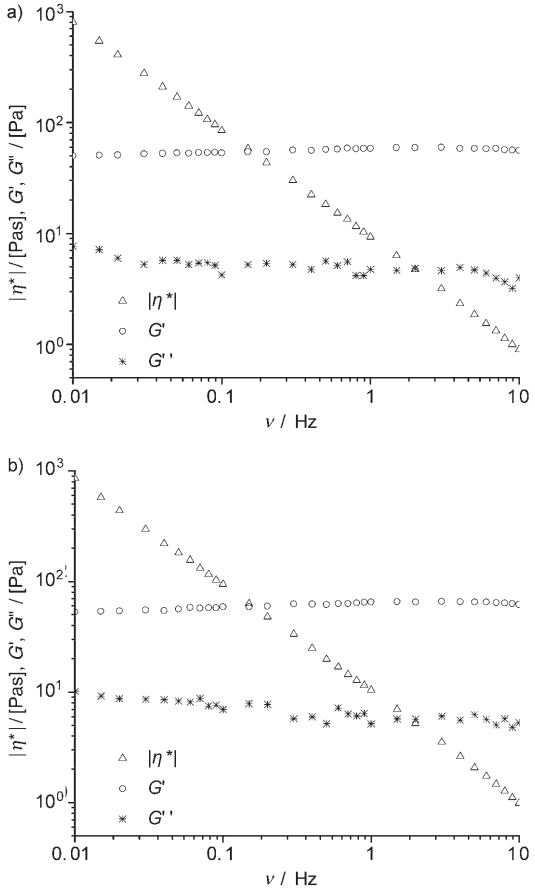

Figure 4. Rheograms of Ca^{2+}– and Ba^{2+}–ligand coordinated vesicles for $100\,mmol\,L^{-1}$ C_{14}DMAO mixed with a) $20\,mmol\,L^{-1}$ $Ca(OA)_2$ or b) $12\,mmol\,L^{-1}$ $Ba(OA)_2$ (b). $T = 25.0 \pm 0.1\,°C$.

phase behavior of the $100\,mmol\,L^{-1}$ C_{14}DMAO/KOA/H_2O system. All the samples are clear solutions, however, the viscosity increases as KOA concentration increases. From the conductivity data shown in Figure 5, one can clearly observe that the conductivity increases linearly over the whole range of KOA concentrations. This result indicates that the K^+ ions are thoroughly disassociated from the surfactant molecules and move freely within the aqueous solutions, which is

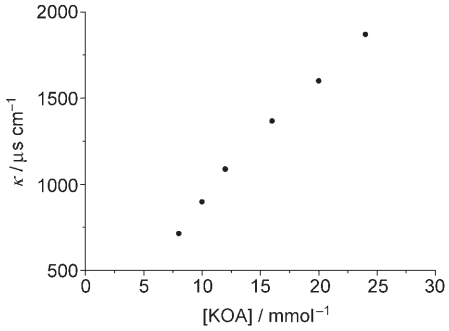

Figure 5. Conductivity as a function of the concentration of KOA in the KOA/C_{14}DMAO/H_2O system. $T = 25.0 \pm 0.1\,°C$.

completely different from the Ca^{2+} and Ba^{2+} systems. The phase behavior shows that the coordination between Ba^{2+}, Ca^{2+}, and the N→O of C_{14}DMAO plays an important role in the formation of vesicles, and that there is no such coordination between K^+ and C_{14}DMAO.

By considering all the results obtained, a formation mechanism of coordinated unilamellar, multilamellar, and oligovesicular vesicles that can satisfy all the experimental measurements and parameters is proposed in Figure 6.

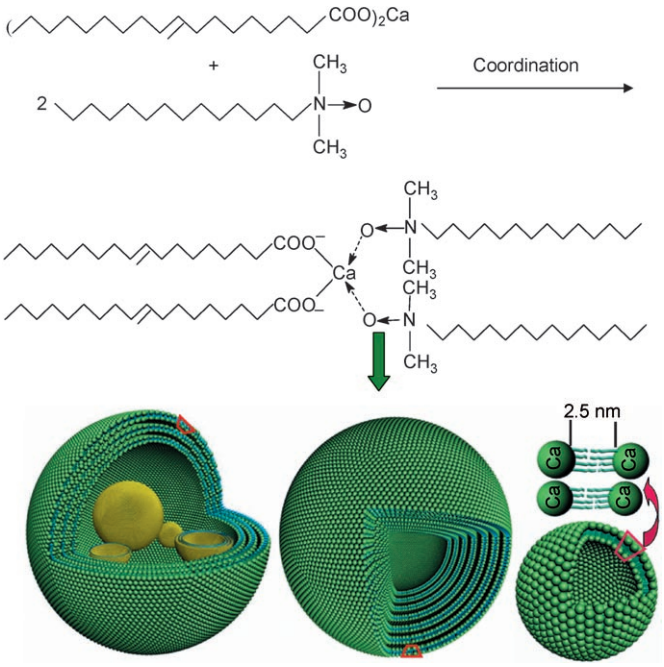

Figure 6. Schematic formation mechanism of unilamellar (right model), multilamellar (middle model), and oligovesicular (left model) vesicles through coordination with Ca^{2+} (or Ba^{2+}). The hydrophobic four-chain hydrocarbons formed by the coordination are shown as blue rods and the hydrophilic-charged Ca^{2+} (or Ba^{2+}) groups as green spheres. A sector in each model has been cut out to enhance visibility. Seven bilayers comprise the multilamellar vesicle phase. In the model of oligovesicular vesicles, four smaller unilamellar and multilamellar vesicles are shown inside, two of the vesicles (one bilayer and one multilamellar) have been cut open and the other two vesicles are shown whole. The thickness of bilayers of around 2.5 nm was determined by fitting SAXS measurements using a lamellar model.

The Ca^{2+}–, Ba^{2+}–ligand coordinated vesicles could be used to produce a vesicle phase of salt-free catanionic surfactants $C_{14}DMAOH^+$–$^-OOC(CH_2)_7CH{=}CH(CH_2)_7CH_3$ in situ. The salt-free catanionic vesicle phase was produced through the hydrolysis of an ester, diethyl oxalate (DO), in situ in C_{14}DMAO/$Ca(OA)_2$/DO or C_{14}DMAO/$Ba(OA)_2$/DO vesicle-phase aqueous solutions.[23] The zwitterionic surfactant C_{14}DMAO can be charged by the H^+ released from oxalic acid ($H_2C_2O_4$), produced by the hydrolysis of diethyl oxalate, to become a cationic surfactant, $C_{14}DMAOH^+$, and Ca^{2+} or Ba^{2+} precipitates as CaC_2O_4 or BaC_2O_4. After the CaC_2O_4 or BaC_2O_4 precipitates are removed from the C_{14}DMAO/$Ca(OA)_2$/DO or C_{14}DMAO/$Ba(OA)_2$/DO solutions, the final mixed solutions do not contain excess salts, unlike other cationic/anionic surfactant systems. Both the C_{14}DMAO/$Ca(OA)_2$ and the C_{14}DMAO/$Ba(OA)_2$ coordination systems and the resulting catanionic $C_{14}DMAOH^+$ –$^-OOC(CH_2)_7CH{=}CH(CH_2)_7CH_3$ solution are birefringent Lα-phase solutions that consist of unilamellar and multilamellar vesicles. Further studies to confirm this point are in progress. This route of vesicle formation solves the problem of how to prepare nanomaterials by using surfactant self-assembly, for which the structure is controlled not by the growing material, but by the phase behavior of the surfactants.

Conclusion

Unilamellar, multilamellar, and oligovesicular vesicles were prepared by Ca^{2+}– and Ba^{2+}–ligand coordination in the mixed aqueous solutions of C_{14}DMAO and $Ca(OA)_2$ or $Ba(OA)_2$. The coordination between C_{14}DMAO and $Ba(OA)_2$ or $Ca(OA)_2$ results in reduction in head-group area and promotes the formation of vesicles. The microstructures of the vesicles were determined by FF-TEM, SAXS, and rheological measurements. The multilamellar vesicles have up to several layers with a thickness of around 2.5 nm. A formation mechanism involving coordination of the metal ions to four hydrophobic surfactant chains, followed by aggregation into vesicles, was proposed. These vesicles can be used to guide the synthesis of nanomaterials by surfactant-controlled growth processes.

Experimental Section

Chemicals: C_{14}DMAO was purchased from Merck and potassium oleate from Fluka. Both were of P.A. quality and were used without further purification. Water was distilled three times. All other reagents used were of P.A. quality.

Experimental methods: $Ca(OA)_2$ and $Ba(OA)_2$ were obtained by adding $CaCl_2$ and $BaCl_2$ solutions into KOA solution dropwise with stirring until Ca^{2+} and Ba^{2+} were in excess. The precipitates formed were filtered and washed until no Ca^{2+} or Ba^{2+} was present in the filtrates, then they were dried at 50 °C for 24 h. The purities of the products were higher than 99 %, as determined by elemental analysis. The Krafft temperatures of $Ca(OA)_2$ and $Ba(OA)_2$ were determined to be above 83 °C and 85 °C, respectively. $Ca(OA)_2$ or $Ba(OA)_2$ (0.050 g) was added to 50 mL water (final concentration 0.1 wt %) and the mixture was stirred by using a magnetic stir bar. The mixture was stirred and heated slowly in a water bath. The Krafft point of $Ca(OA)_2$ or $Ba(OA)_2$ was the temperature at which all the solid surfactant had dissolved into solution.

The samples were obtained by dissolving various amounts of $Ca(OA)_2$ or $Ba(OA)_2$ in 100 mmol L^{-1} C_{14}DMAO solutions under sonication. The solutions were allowed to equilibrate for at least four weeks at 25.0 ± 0.1 °C until they remained unchanged. The phase diagram was obtained by observing the solutions in calibrated test tubes at the same temperature of 25.0 ± 0.1 °C.

The conductivity measurements of the samples were obtained by using a DDSJ-308 A conductivity meter (Lei-ci, Shanghai, China) at 25 °C. The two-phase solutions were detected under stirring so that only one result was obtained for each sample.

Rheological measurements were carried out by using a RS 75 stress-controlled rheometer (Haake company) using a cone-plate measuring system. The lowest possible stress value was 3 mPa. The viscoelastic properties of the samples were determined by recording the oscillatory measurements from 0.01 to 10 Hz, at which either the strain amplitude or the stress amplitude can be kept constant.

For the FF-TEM, a small amount of sample was placed on a 0.1-mm-thick copper disk and covered with a second copper disk. The copper sandwich containing the sample was frozen by plunging it into liquid propane that had been cooled in liquid nitrogen. Fracturing and replication were carried out by using a freeze-fracture apparatus (Balzers BAF 400, Germany) at −140 °C. Pt/C was deposited at an angle of 45°. The replicas were examined by using a JEOL's TEM 100cx II (Japan) at an accelerating voltage of 100 kV.

Small-angle X-ray scattering (SAXS) measurements were carried out at RT by using a modified Kratky compact camera. The evacuated camera was mounted on a sealed X-ray tube equipped with a copper target. The scattering intensities were measured by using a linear position-sensitive, gas-filled detector (Mbraun, Germany) by monitoring the scattering curves in the q range ($q=4\pi/\lambda\sin\frac{\theta}{2}$, in which θ is the scattering angle and λ is the wavelength of the radiation). The sample solutions were injected into a 1-mm-diameter quartz capillary mounted in a steel cuvette. The data collection time for each scattering curve was about 15 h.

Acknowledgements

This work was supported by the NSFC (20473049, 20571048, 20533050, 20428101); the Program of Hundreds of Talents of the Chinese Academy of Sciences; the Specialized Research Fund for the Doctoral Program of Higher Education (20050422009), and the NSF, Shandong Province (Z2004B04). The authors thank Dr. Pamela D. Holt, Shandong University, for assistance with the manuscript.

[1] Y. Chevalier, Th. Zemb, *Rep. Prog. Phys.* **1990**, *53*, 279–371.
[2] D. H. W. Hubert, M. Jung, A. L. German, *Adv. Mater.* **2000**, *12*, 1291–1294.
[3] R. G. Laughlin, *The Aqueous Behavior of Surfactants*, Academic press, London, **1994**.
[4] J. Israelachvili, D. J. Mitchell, B. W. Ninham, *J. Chem. Soc. Faraday Trans. 2* **1976**, *72*, 1525–1568.
[5] J. N. Israelachvili, *Intermolecular and Surface Forces*, 2nd ed., Academic press, **1991**.
[6] a) R. P. Sijbesma, F. H. Beijer, B. J. B. Folmer, J. H. K. K. Hirschberg, R. F. M. Lange, J. K. L. Lowe, E. W. Meijer, *Science* **1997**, *278*, 1601–1604; b) L. Brunsveld, B. J. B. Folmer, E. W. Meijer, R. P. Sijbesma, *Chem. Rev.* **2001**, *101*, 4071–4098; c) K. Yamauchi, J. R. Lizotte, D. M. Hercules, M. J. Vergne, T. E. Long, *J. Am. Chem. Soc.* **2002**, *124*, 8599–8604.
[7] S. Park, J. H. Lim, S. W. Chung, C. A. Mirkin, *Science* **2004**, *303*, 348–351.
[8] E. W. Kaler, A. K. Murthy, B. E. Rodriguez, J. A. N. Zasadzinski, *Science* **1989**, *245*, 1371–1374.
[9] H. T. Jung, B. A. Coldren, J. A. Zasadzinski, D. J. Iampietro, E. W. Kaler, *Proc. Natl. Acad. Sci. USA* **2001**, *98*, 1553–1557.
[10] H. T. Jung, Y. S. Lee, E. W. Kaler, B. A. Coldren, J. A. Zasadzinski, *Proc. Natl. Acad. Sci. USA* **2002**, *99*, 15318–15322.
[11] B. A. Coldren, H. Warriner, R. van Zanten, J. A. Zasadzinski, E. B. Sirota, *Proc. Natl. Acad. Sci. USA* **2006**, *103*, 2524–2528.
[12] J. Hao, H. Hoffmann, *Curr. Opin. Colloid Interface Sci.* **2004**, *9*, 279–293.
[13] Th. Zemb, M. Dubois, B. Demé, Th. Gulik-Krzywicki, *Science* **1999**, *283*, 816–819.
[14] M. Dubois, B. Demé, Th. Gulik-Krzywicki, J. C. Dediu, C. Vautrin, S. Désert, E. Perez, Th. Zemb, *Nature* **2001**, *411*, 672–675.
[15] M. Dubois, V. Lizunov, A. Meister, Th. Gulik-Krzywicki, J. M. Verbavatz, E. Perez, J. Zimmerberg, Th. Zemb, *Proc. Natl. Acad. Sci. USA* **2004**, *101*, 15082–15087.
[16] A. Song, S. Dong, X. Jia, J. Hao, W. Liu, T. Liu, *Angew. Chem.* **2005**, *117*, 4086–4089; *Angew. Chem. Int. Ed.* **2005**, *44*, 4018–4021.
[17] a) J. Hao, J. Wang, W. Liu, R. Abdel-Rahem, H. Hoffmann, *J Phys Chem. B* **2004**, *108*, 1168–1172; b) J. Wang, A. Song, X. Jia, J. Hao, W. Liu, H. Hoffmann, *J. Phys. Chem. B* **2005**, *109*, 11126–11134.
[18] a) A. Zapf, R. Bech, G. Platz, H. Hoffmann, *Adv. Colloid Interface Sci.* **2003**, *100–102*, 349–380; b) R. Beck, Y. Abe, T. Terabayashi, H. Hoffmann, *J. Phys. Chem. B* **2002**, *106*, 3335–3338; c) A. Zapf, U. Hornfeck, G. Platz, H. Hoffmann, *Langmuir* **2001**, *17*, 6113–6118; d) H. Hoffmann, D. Gräbner, U. Hornfeck, G. Platz, *J. Phys. Chem. B* **1999**, *103*, 611–614.
[19] J. Hao, H. Hoffmann, K. Horbasck, *Langmuir* **2001**, *17*, 4151–4160.
[20] P. Lindner, Th. Zemb, *Neutrons, X-rays and Light: Scattering Methods Applied to Soft Condensed Matter*, North-Holland Delta Series, Elsevier, Amsterdam, **2002**.
[21] G. Porod in *Small-angle X-ray scattering* (Eds.: O. Glatter, O. Kratky), Academic Press, London, **1982**.
[22] P. Alexandridis, U. Olsson, B. Lindman, *Langmuir* **1998**, *14*, 2627–2638.
[23] J. I. Escalante, H. Hoffmann, *J. Phys.: Condens. Matter* **2000**, *12*, A483–A489.

Received: March 13, 2006
Published online: September 22, 2006

